Popular Summary of "On Magnetic Spectra of Earth and Mars"

by C. V. Voorhies 1/15/02

C. V. Voorhies[1], T. J. Sabaka[2], and M. Purucker[2]
[1]Geodynamics Branch, NASA, Goddard Space Flight Center, Greenbelt, MD
[2]Raytheon ITSS at Geodynamics Branch, Goddard Space Flight Center, Greenbelt, MD.
Accepted for Publication in the Journal of Geophysical Research - Planets

When astrophysicists measure light from a distant star, they can break up the starlight into its component colors, creating a spectrum from long wavelength red to short wavelength blue, by beaming the light through a mechanical prism. Similarly, when geophysicists measure a planet's magnetic field, they can break up the field into long and short wavelength components by running the data through a kind of digital prism called "spherical harmonic analysis." And much as astrophysicists can say much about a star's surface and interior from its optical spectrum, geophysicists can infer something about a planet's crust and core from its magnetic spectrum.

Earth's magnetic spectrum is determined from measurements made at magnetic observatories, along land, ocean, or aero-magnetic survey lines, and from global satellite magnetic surveys such NASA's Magsat and Denmark's Oersted satellite. Mars' magnetic spectrum can now be determined from measurements made by NASA's Mars Global Surveyor.

Earth's magnetic spectrum shows both a powerful, long-wavelength, core-source magnetic field, caused by electric current in its liquid iron outer core, and a short-wavelength crustal-source field, caused by magnetization of crustal rock. For Mars, however, there is no sign of a core-source field. Moreover, the traditional model for interpreting the geomagnetic spectrum does not work for Mars. Fortunately, A new theoretical model of planetary magnetic spectra, developed for Earth's crust, also works well for Mars.

The new spectral method for distinguishing crustal from core-source magnetic fields has now been applied to both Earth and Mars. The spectra are fairly fitted by theoretical forms expected from certain elementary classes of magnetic sources. For Earth we find fields from a core of radius 3512 ± 64 km, in accord with the seismologic core radius of 3480 km, and from a crust represented by a shell of random dipolar sources at radius 6367 ± 14 km, near Earth's mean radius of 6371.2 km. For Mars we find no sign of a core-source field, only a field from a crust represented *in same way*, but at radius 3344 ± 10 km, about 46 km below Mars' mean radius of 3390 km, and with sources about 9.6 ± 3.2 times stronger than Earth's.

The magnetic crustal shell depth agrees well with the mean depth of Mars lithosphere inferred by independent analysis of independent MGS topography and gravity data.

Our results indicate Mars has a thicker, more intensely magnetized crust than Earth. This may in part be due to an iron-rich crustal magnetic mineralogy for the Red Planet, magnetized by a now defunct core-dynamo. Curiously, owing to its strong, short-wavelength magnetic anomalies, the Red Planet has a much 'bluer' magnetic spectrum than the Blue Planet.

On Magnetic Spectra of Earth and Mars

C. V. Voorhies[1], T. J. Sabaka[2], and M. Purucker[2]
[1]Geodynamics Branch, NASA, Goddard Space Flight Center, Greenbelt, MD
[2]Raytheon ITSS at Geodynamics Branch, Goddard Space Flight Center, Greenbelt, MD.
Revised for Journal of Geophysical Research - Planets (Version 12/6/01)

Abstract: The spectral method for distinguishing crustal from core-source magnetic fields is re-examined, modified, and applied to both a comprehensive geomagnetic field model and an altitude normalized magnetic map of Mars. The observational spectra are fairly fitted by theoretical forms expected from certain elementary classes of magnetic sources. For Earth we find fields from a core of radius 3512 $\pm$ 64 km, in accord with the seismologic core radius of 3480 km, and a crust represented by a shell of random dipolar sources at radius 6367 $\pm$ 14 km, near the planetary mean radius of 6371.2 km. For Mars we find no sign of a core-source field, only a field from a crust represented in same way, but at radius 3344 $\pm$ 10 km, about 46 km below the planetary mean radius of 3389.5 km, and with sources about 9.6 $\pm$ 3.2 times stronger.

1. INTRODUCTION

Geophysical interpretations of planetary magnetic field measurements may differ because knowledge of the field outside a planet alone does not uniquely determine the distribution of magnetic sources inside the planet. Physical constraints on possible sources reduce such non-uniqueness, as do mathematical restrictions on the source distributions considered. With enough restrictions, one of the many source distributions that are equivalent to, or at least closely fit, the measured field can be determined.

Such a deterministic field model may aid mapping, interpolation, separation of fields originating outside the planet, noise reduction, and interpretation. Because it represents the field from internal sources, if not the true sources themselves, a deterministic model might also be combined with statistical models of source distributions to make some inferences about the sources. As an exercise in comparative planetology, we combine deterministic and statistical approaches to the magnetic fields of Earth and Mars.

In practice, after correcting for external sources, a terrestrial field that varies over broad length scales is often attributed to electric current in Earth's core, subtracted from near surface geomagnetic measurements, and the residual, narrower scale, field attributed to magnetization of Earth's crust and lithosphere. Separation of crustal from core-source fields based on length scale may also be attempted in the spectral wavenumber domain of a Fourier-Fourier transformed regional magnetic survey or a Fourier-Legendre (spherical harmonic) model of the global magnetic field. Among such separations, perhaps the most widely accepted are those based on spherical harmonic analyses of Magsat data by *Langel & Estes* [1982] and by *Cain et al.* [1989b].

Here we re-examine spectral separation of core from crustal-source fields, adopt some modifications suggested by theoretical consideration of planetary crustal sources, and apply them to both a comprehensive geomagnetic field model [*Sabaka, Olsen & Langel,* 2000] and an altitude normalized magnetic map of Mars [*Purucker et al.*, 2000].

2. BACKGROUND AND NOTATION

Consider magnetic flux density $\boldsymbol{B}$ at time t and position $\boldsymbol{r}$ in planet centered spherical polar coordinates (r, θ, ϕ) due to amperian currents and magnetization within a reference sphere of radius a. Above this sphere, solenoidal $\boldsymbol{B}(\boldsymbol{r},t)$ can be represented as the negative gradient of an internal scalar magnetic potential $V(\boldsymbol{r},t)$ such that $\boldsymbol{B} = -\nabla V$. The potential satisfies Laplace's equation and has well-known spherical harmonic expansion

$$V = a \sum_{n=1}^{\infty} (a/r)^{n+1} \sum_{m=0}^{n} [g_n^m(t)\cos m\phi + h_n^m(t)\sin m\phi] P_n^m(\cos\theta) , \qquad (1)$$

where $[g_n^m, h_n^m]$ denote the Gauss coefficients, and P_n^m denotes the Schmidt normalized associated Legendre polynomial, of integer degree n and order m. Coefficients through finite degree N can be estimated by fitting the gradient of a truncated expansion to measured planetary magnetic data (see, *e.g.*, *Langel* [1987]). Harmonic representation (1) is equivalent to a planet centered multipole moment expansion. It is used for efficiency, not physical plausibility: planet centered point multipoles are not true sources.

The mean square magnetic field described by harmonics of degree n, averaged over a spherical surface of radius r containing the sources, is given by

$$R_n(r,t) = (n+1)(a/r)^{2n+4} \sum_{m=0}^{n} ([g_n^m(t)]^2 + [h_n^m(t)]^2) \qquad (2)$$

(see, *e.g.*, *Lowes* [1966]). As a function of n, R_n forms a discrete (line) spectrum called the spatial magnetic power spectrum of the planet. Although R_n has units of (Tesla)^2, the magnetic energy density per harmonic degree integrated over the surface, which is just $2\pi r^2 R_n/\mu_0$ in vacuum permeability μ_0, indeed has units of spatial power (J/m) or force (N). Each individual R_n represents a centered multipole power (*e.g.*, dipole power R_1, quadrupole power R_2, hexapole power R_3, *etc.*). Reliable estimates of R_n for either Earth or Mars are, at present, available only for degrees less than 100, and perhaps less than 50.

As averages over a centered sphere, multipole powers are invariant under coordinate system rotations. This is not true for translations, as exemplified by the spectrum due to a single point dipole of vector moment $\boldsymbol{m} \equiv \boldsymbol{M}/\mu_0$ offset to position $\boldsymbol{r}_x$

$$R_n^{SD}(r) = (4\pi r^3)^{-2} (r_x/r)^{2n-2} [n^2(n+1)M_r^2 + n(n+1)^2(M_\theta^2 + M_\phi^2)/2] \qquad (3)$$

(see, *e.g.*, *Voorhies* [1998]). There is no radius $r > r_x > 0$ at which the attenuated cubic spectrum (3) becomes independent of n. Moreover, a well offset radial dipole produces almost twice the power of a similarly offset horizontal dipole of equal absolute moment. The single area of very strong field directly above the radial dipole contributes more to the mean square field than the two areas of strong field somewhat further from the horizontal dipole due to the anisotropic inverse cube law for dipolar fields.

3. THEORETICAL CRUSTAL MAGNETIC SPECTRA

Now consider a large number of dipoles with random moments $\boldsymbol{M}^k$ ($k = 1,2,3, \ldots K$) scattered on a sphere of radius r_x. Dipole positions $\boldsymbol{r}_k$ amount to random samples of a laterally uniform distribution and are thus expected to be laterally uncorrelated: $\{\boldsymbol{r}_k \bullet \boldsymbol{r}_{k'}\} = r_x^2 \delta_{kk'}$, where curly brackets denote expectation value and Kroenecker $\delta_{kk'}$ is unity if $k = k'$ and is otherwise zero. For randomly oriented dipoles, any particular orientation is as likely as its opposite and there is no reason to expect either cross-correlated components for any individual moment or cross-correlated moments between different dipoles; however, auto-correlations remain perfect. With components of $\boldsymbol{M}^k$ denoted M_i^k ($i = r$, θ, or ϕ), the expected situation is summarized via zero mean dipole moments of diagonal covariance:

$$\{M_i^k\} = 0 \tag{4a}$$

$$\{M_i^k M_{i'}^{k'}\} = \delta_{ii'} \delta_{kk'} \{M^2\}/3 , \tag{4b}$$

where $\{M^2\}$ is the mean square moment of the K dipoles. Although the expectation value of the vector field above the spherical shell is zero, the expected field intensity is not. Indeed, the spatial magnetic power spectrum expected from a spherical shell of such randomly oriented dipoles is just the sum of individual spectra (3):

$$\{R_n(r)\}^{ss} = \frac{K\{M^2\}}{3(4\pi r^3)^2}\, n(n+1)(2n+1)\left(\frac{r_x}{r}\right)^{2n-2} \tag{5a}$$

$$= A_x\, n\,(n+\tfrac{1}{2})(n+1)(r_x/a)^{2n-2}\,(a/r)^{2n+4}\,, \tag{5b}$$

where $A_x \equiv (2/3)K\{M^2\}(4\pi a^3)^{-2}$. The root sum square (rss) magnetic dipole moment per unit area $(K\{M^2\})^{1/2}(4\pi\mu_0 r_x^2)^{-1}$ has units of Ampere-turns and equals $(3A_x/2)^{1/2}(a^3/\mu_0 r_x^2)$.

Extrema of (5) with respect to n are readily calculated; there is typically a spectral maximum near degree $3/[2\ln(r/r_x)]$. For example, at terrestrial reference radius $r = a_E = 6371.2$ km, a shell depth $(a_E - r_x)$ of either 10, 20, or 40 km gives a spectral peak at degree 954, 477, or 238, respectively. At the 3389.5 km mean radius of Mars [*Smith et al.,* 1999], a shell depth of 20, 50, or 100 km gives a peak at degree 253, 100, or 50, respectively.

Of course, the magnetic field from a real planetary crust includes the superposition of fields originating in a very large number of very small rock magnetic domains. Well above the crust, the field from each domain is closely approximated by that from a point dipole. At an instant in geologic time, these crustal sources may thus be regarded as a sample of an ensemble of dipole distributions. If a small scale geologic structure has a fairly uniform magnetization which differs from that of the country rock, then its field can be approximated by that of domain dipoles which are strongly correlated over the few km size of the structure. (Examples might include a granite batholith, andesite diapir, basalt flow, salt dome, or metamorphic lens in Earth, or a hematite-rich dune, knob, or small crater on Mars). To treat domain dipoles as if randomly oriented would thus seem to neglect coherently magnetized geologic structure and focus on background noise. Yet when measured *at satellite altitudes* of a few hundred km, the field from such a localized structure should be well represented by a single point dipole. When such measurements are

represented in terms of expansion (1), many compact crustal-source contributions to low degree multipole powers (2) should thus be fairly well approximated by (5).

When the field well above a cluster of nearby, roughly vertical sources at a given depth is fitted with but one dipole, the strongest field and its fall off with altitude tend to be more closely fitted by placing the single stronger dipole at greater depth. The extra strength and depth shift spatial magnetic power from higher to lower degrees by (3). Use of spectrum (5) may similarly overestimate the true depth of laterally correlated sources.

Significant lateral source correlation over broad scale geologic provinces (such as an orogenic belt, subduction zone, continental shield, or ocean basin on Earth, or a highland or large impact basin on Mars) suggests substantial deviations from (5), perhaps by a factor of two or more. Relative to a decorrelated crust giving the same mean square field at a given altitude, such broad structure is also thought to shift spatial power from higher to lower degrees. Real geologic structures may thus produce a more nearly exponential magnetic spectrum than (5), perhaps an attenuated quadratic in n; however, it is not yet clear that the purely exponential form assumed by *Langel & Estes* [1982] and *Cain et al.* [1989b] is expected from magnetic sources distributed in a roughly oblate spheroidal layer with heterogeneous, scale-variant, and anisotropic two-point correlation functions. As shown below, crustal thickness, oblateness, source polarization and correlation do change (5) in ways that can be critical to its application and interpreting results.

3.1 Randomly Magnetized Oblate Spheroidal Layers

Variations of spectrum (5) have been derived to account for layer thickness, ellipticity, sources aligned by a reversing main field, and all combinations thereof [*Voorhies*, 1998]. For a thick spherical layer, or spherical annulus, of randomly oriented (and positioned) dipoles, the expectation spectrum is that obtained by *Jackson* [1990], here written

$$\{R_n(r)\}^{sa} = A_x^I (2\pi a^3/X)\, n\,(n+1)\left[\left(\frac{r_x + d}{a}\right)^{2n+1} - \left(\frac{r_x - d}{a}\right)^{2n+1}\right](a/r)^{2n+4}, \qquad (6)$$

where $2d$ denotes layer thickness; $r_x - d$ is the inner, and $r_x + d$ the outer, radius of the annulus; and X represents the annular volume.

For a thin layer with $2d/r_x << 1$, the thickness factor (the ratio of (6) to (5)) becomes important for degrees near or exceeding $r_x/2d$. For example, with $r_x + d$ set to a_E and $2d$ set to 40 km, $r_x/2d$ is 159 and the thickness factor is but 1.10 at degree 120; yet it increases to 2.10 at degree 360 and reaches 10.2 at degree 720. At lower degrees the square bracketed term is approximately $(2n+1)(2d/r_x)(r_x/a)^{2n+1}$, so partial derivatives of (6) with respect to thickness are approximately proportional to partials with respect to amplitude. Amplitude and thickness may thus be nearly colinear, hence virtually inseparable from a low degree observational spectrum alone: an increase in magnetization amplitude can be compensated by a decrease in layer thickness and *vice versa*.

For thick layers or high degrees $n >> r_x/2d$, expectation spectrum (6) approaches an exponentially attenuated quadratic in n instead of the cubic (5); indeed, for a ball of random dipoles ($r_x = d = a/2$) it is proportional to $n(n+1)[(r_x+d)/r]^{2n+4}$. Effects of lateral source correlation on R_n might thus be mistaken for those of a very thick layer; alternately, the spectrum from a ball of random dipoles might be used as a proxy for such effects.

Because neither (1) nor (2) represent sources above the reference sphere, partial sums of a spectrum evaluated on too small a sphere may diverge due to the ellipticity and topography of a magnetized planetary crust (*e.g.*, magnetization of Mount Kilimanjaro if not Olympus Mons). For example, consider an ellipsoidal shell of semi-major axis a_x, semi-minor axis b_x, volume

$\pi a_x^2 b_x$, eccentricty ε ($\varepsilon^2 \equiv 1 - (b_x/a_x)^2$), and area $A_e = 2\pi a_x^2 + \pi b_x^2 \varepsilon^{-1} \ln[(1+\varepsilon)/(1-\varepsilon)]$. The spatial magnetic power spectrum expected from randomly oriented dipoles scattered on such an oblate spheroidal shell is

$$\{R_n(r)\}^{es} = (4\pi r_x^2/A_e)\,(a_x/r_x)^{2n}\,Q_n\,\{R_n(r)\}^{ss}, \tag{7a}$$

where $\{R_n(r)\}^{ss}$ on the right is from (5) and, in terms of $\gamma^2 = (a_x/b_x)^2 - 1$ (dubbed "coeccentrcity") and parameter $\alpha^2 = 2\gamma^2 + \gamma^4$,

$$Q_n = \int_0^1 (1 + \gamma^2 x^2)^{-n-1} [1 + \alpha^2 x^2]^{1/2}\, dx\,. \tag{7b}$$

For terrestrial γ^2 [*Nerem, et al.,* 1994], Q_n decreases from 0.97 at degree 12 to 0.36 at degree 900; however, if (7a) is evaluated at $r = a_E < a_x$, the factor $(a_x/a_E)^{2n}$ increases from 1.06 to 91.4. Elevation of randomly oriented dipoles on the equatorial bulge thus contributes more to the expectation spectrum than is removed by depressing such sources near the poles. As anticipated, the ellipticity factor (the ratio of (7a) to (5b)) becomes important at degrees near or exceeding the reciprocal flattening $a_x/(a_x - b_x)$. For Earth, this factor is 1.166 or more for $n > 298$; yet Mars' flattening is 1/170 [*Smith et al.,* 1999].

Finally, consider an oblate spheroidal annulus of invariant eccentricity, hence variable thickness. At the top of the layer $r^2(\theta) = a_x^2(1 + \gamma^2\cos^2\theta)$; at the base of the layer of equatorial thickness $2d$, $r^2(\theta) = (a_x - 2d)^2(1 + \gamma^2\cos^2\theta)$. The spectrum expected from random dipoles (4) distributed uniformly throughout such an ellipsoidal annulus is

$$\{R_n(r)\}^{ea} = A_x^I\,(2\pi a^3/X_{ea})\,n(n+1)\,W_n\left(\frac{a_x}{a}\right)^{2n+1}\left[1 - \left(\frac{a_x - d}{a_x}\right)^{2n+1}\right](a/r)^{2n+4}\,, \tag{8a}$$

where X_{ea} denotes annular volume $4\pi a_x b_x (2d)[1 + 2d/a_x - (2d^2/a_x)^2/3]$ and

$$W_n = \int_0^1 (1 + \gamma^2 x^2)^{-n-1} \left[\frac{1 + \alpha^2 x^2}{1 + \gamma^2 x^2}\right]^{1/2} dx . \qquad (8b)$$

For thin layers of small eccentricity, the ratio of spectra (8a) to (5a) is approximately the product of thickness and ellipticity factors. For a layer of 52 km equatorial thickness and the coeccentricty of Mars, the exact ratio reaches 1.41 at degree 90 (still less than a factor of 2).

3.2 Random Polarity Shells and Layers

Thermoremanent magnetization (TRM) of igneous rock cooling in a planet centered axial dipole field that can reverse polarity suggests non-randomly oriented domain dipoles. Post-TRM reorientation of domains by crustal deformation, sea-floor spreading, and continental drift; metamorphic remagnetization; true polar wander; and erosion may arguably lead to a terrestrial crustal spectrum more akin to that of randomly oriented dipoles than random polarity dipoles. Yet contrasts in magnetic susceptibility still indicate a main field aligned component of induced magnetization in Earth's crust. Magnetic spectra for ensembles of offset, uncorrelated dipoles aligned either parallel or anti-parallel to a centered dipole field [*Voorhies*, 1998] are thus summarized physically as follows.

The ratio of the spectrum expected from such random polarity dipoles on a shell to spectrum (5b) is $(5/4)(n + 1/5)/(n + ½)$, provided $K\{M^2\}$ and r_x are the same. All else being equal, multipole powers from random polarity dipoles are about 25% more than from randomly oriented dipoles. This is attributed to the near radial orientation and typically strong moments $\{2M^2\}^{1/2}$ of field-aligned dipoles located near the poles. This surplus power from the polar

regions evidently exceeds the deficit due to the nearly horizontal orientation and typically weak moments $\{M^2/2\}^{1/2}$ of sources near the equator.

For a thin spherical annulus, variations of field aligned sources with depth due to the small change in the centered dipole field with depth are omitted along with deviations of the polarizing main field from a planet centered dipole. The ratio of the expected spectrum from random polarity dipoles in a spherical annulus to that from such sources on a shell is then same as the ratio of spectra (6) to (5). This thickness factor remains near unity for degrees less than the radius-to-thickness ratio of the annulus.

Curiously, the ellipticity factor for random polarity dipoles on an oblate spheroidal shell can be less than unity for low to intermediate degrees. This is because the stronger, nearly radial domain dipoles near the flattened poles are now further from a source containing sphere on which R_n is evaluated. As expected, the corrections are appreciable at degrees near or exceeding the reciprocal flattening (*e.g.*, -18% at n = 300 in the terrestrial case). At sufficiently high degrees (*e.g.*, 720), however, the ellipticity factor again exceeds unity. The spectrum expected from random polarity dipoles distributed uniformly throughout an oblate spheroidal annulus can be closely approximated by the product of thickness and ellipticity correction factors.

3.3 Spectrum of a Vertically Correlated Crust

Inversions of magnetic data for parameters describing magnetized slabs or equivalent-source shells are often discussed in terms of "magnetization times thickness". This refers to a *vertically correlated*, typically uniform, magnetization. Shell spectra (5) or (7) amount to the simultaneous limits of vanishing thickness and singular magnetization, so they should approximate the spectrum from a single, vertically correlated layer of magnetic material, provided the layer is very thin and its magnetization varies over similarly small lateral scales. In contrast, spectra (6)

and (8) assume vertically, as well as laterally, decorrelated sources; such spectra from a thick, heterogeneously magnetized layer do not describe, and ought not be mistaken for, that from a uniformly magnetized layer. Indeed, a random polarity layer spectrum may well approximate that from a thick crust composed of sequences of thin, localized volcanic flows and sills recording many main field polarity reversals.

To derive the spectrum expected from a spherical annulus of vertically correlated, yet laterally uncorrelated, sources, we assign each domain dipole a lateral position index k as before and, at each k, a radial position index $j = 1, 2, 3, \ldots J$ for each radius in the range $[r_x\text{-d}, r_x\text{+d}]$. The sum squared magnetic dipole moment becomes $KJ\{M^2\}/\mu_0^2$, but lateral decorrelation rules (4) still apply and yield

$$\{R_n(a)\}^{VCL} = \frac{K\{M^2\}}{3(4\pi a^3)^2}\,[n(n+1)(2n+1)]\,\{\sum_{j=1}^{J}\sum_{j'=1}^{J}\left(\frac{r_j\, r_{j'}}{a^2}\right)^{n-1}\}. \qquad (9a)$$

Each sum in (9a) amounts to J times the mean value of terms. This mean is expected to equal the volume weighted integral for random samples of a uniform distribution. The sums over discrete radii are therefore replaced by integrals through the layer, which gives

$$\{R_n(a)\}^{VCL} = \frac{KJ^2\{M^2\}}{3X^2}\,\frac{n(n+1)(2n+1)}{(n+2)^2}\,\left[\left(\frac{r_x+d}{a}\right)^{n+2} - \left(\frac{r_x-d}{a}\right)^{n+2}\right]^2, \qquad (9b)$$

where X remains the annular volume. For a relatively thin layer ($r_x/d << n$ and X^2 proportional to d^2), the squared bracketed term is approximately $4d^2(n+2)^2(r_x/a)^{2n+4}$; therefore, the ratio of spectra (9) to (5) only differs appreciably from a constant at degrees approaching r_x/d or more. (To recover (5a), treat the sums in (9a) as if zero unless j equals j'; to recover (6a), collapse them into one sum replaced by one integral).

3.4 Spectrum of a Laterally Correlated Structure

Consider a magnetized spherical cap at radius r_x with half angle θ_o, non-zero uniform radial sheet magnetization S_r/μ_o only for $\theta \leq \theta_o$, and area $A_c = 2\pi r_x^2(1 - \cos\theta_o)$. If this sheet magnetization represents an array of L radial domain dipoles of identical moments M_r/μ_o, then $S_r = LM_r [2\pi r_x^2(1 - \cos\theta_o)]^{-1}$ and the total moment of the cap is $S_r A_c = LM_r$. Gauss coefficients are easily evaluated for a cap centered on the north pole; however, the magnetic spectrum from a uniformly magnetized spherical cap (MSC), being invariant under rotations, does not depend on the location of the cap on the sphere and is given by

$$[R_n(r;\theta_o)]^{MSC} = (LM_r/4\pi r^3)^2 (r_x/r)^{2n-2} (n/2)[Z_n(\theta_o)]^2 . \tag{10a}$$

The dependence on cap angle is contained in the regular polynomial denoted

$$Z_n(\theta_o) \equiv \left[\frac{\sin\theta_o \; P_n^1(\cos\theta_o)}{(1 - \cos\theta_o)}\right] = [n(n+1)/2]^{-1/2}(1 + x_o)[dP_n^0(x_o)/dx_o] , \tag{10b}$$

where $x_o \equiv \cos\theta_o$. In the limit as θ_o approaches zero, the cap approaches a point radial dipole, Z_n approaches $[2n(n+1)]^{1/2}$, and spectrum (10a) approaches (3).

For a very small cap, we can expand $Z_n(x_o)$ in a finite Taylor series about the pole. Well-known properties of Legendre polynomials P_n^0 allow us to write this expansion in $\Delta x = x_o - 1 \leq 0$ as a normalized deviation from the point dipole value $Z_n(1)$,

$$\frac{Z_n(x_o) - Z_n(1)}{[2n(n+1)]^{1/2}} = \sum_{j=1}^{n} \frac{(\Delta x)^j}{(j+1)!} \prod_{k=1}^{j} \frac{n(n+1) - k(k-1)}{2k} . \tag{11}$$

Provided $|\Delta x| < 4/[n(n+1)]$, successive terms in summed sequence (11) alternate sign and have monotonically decreasing absolute values. This is also the condition for the absolute value of the

first term in the sequence to be less than one. This condition fails for $n \geq n^*$, where $n^*(n^* + 1) \equiv (8\pi r_x^2/A_c)$. Near and above degree n^*, the magnetic spectrum from the cap therefore departs from that of a point dipole, even for a small cap (with $1 - \cos\theta_o \approx \theta_o^2/2$ and $n^* = [4/(1 - \cos\theta_o)]^{1/2} \approx 8^{1/2}/\theta_o$). Physically, edge effects associated with spatial resolution of the cap via harmonics near and above degree n* cause the spectrum to oscillate with Z_n^2 between values near zero and local maxima. For a $(1000\ \text{km})^2$ cap, n^* would be about 31 on Earth and 16 on Mars.

At very high degrees $n >> 1$, the ringing spectrum from a resolved cap $n\theta_o > 1$ can be described via the asymptotic series for P_n^o (see, *e.g.*, *Gradshtyn & Ryzhik* [1994]). The leading term in the series is, using Stirling's approximation, just Laplace's formula

$$P_n^o(\cos\theta_o) = (2/n\pi\sin\theta_o)^{1/2} \cos[(n + \tfrac{1}{2})\theta_o - \pi/4] + O(n^{-3/2}) . \tag{12a}$$

We substitute the derivative of (12a) into (10b) to obtain the asymptotic relation

$$Z_n(\theta_o;\, n >> 1) = [n(n+1)/2]^{-1/2}(1+\cos\theta_o)[(n\pi\sin^3\theta_o/2)^{-1/2}(n + \tfrac{1}{2})\sin[(n + \tfrac{1}{2})\theta_o - \pi/4] + O(n^{-1/2})]. \tag{12b}$$

The asymptotic cap spectrum, obtained by substituting (12b) into (10a), contains the factor $\sin^2[(n + \tfrac{1}{2})\theta_o - \pi/4]$. Because this factor is at most unity, the upper envelope of local asymptotic spectral maxima for $n >> 1$ and non-negligible $\theta_o > 1/n$ is, to order n^{-1} accuracy, given by the plain exponential

$$[R_n(r;\theta_o;n>>1]^{MSC} \leq (LM_r/4\pi r^3)^2 (r_x/r)^{2n-2} [(n + \tfrac{1}{2})^2/n(n+1)](1+\cos\theta_o)^2[2/(\pi\sin^3\theta_o)] \tag{13a}$$

$$\leq (LM_r/4\pi r^3)^2 (r_x/r)^{2n-2}\, 2(1+\cos\theta_o)^2/(\pi\sin^3\theta_o) \tag{13b}$$

$$\leq (S_r\, r_x^2/2r^3)^2 (r_x/r)^{2n-2}\, (2/\pi)\sin\theta_o . \tag{13c}$$

Even for a small cap ($\sin\theta_o \approx \theta_o$), the envelope (13b) of the asymptotic spectrum falls well below the attenuated cubic from a point dipole; indeed, the ratio of envelope (13b) to spectrum (3) for a single radial dipole of the same total moment is then just $8/[\pi n^3 \theta_o^3]$.

3.5 A Laterally Correlated Crustal Magnetic Spectrum

The total spectrum expected from many independent (uncorrelated) magnetized spherical caps of various areas A_i and various total moments is just the sum of individual cap spectra. This sum may be replaced with integrals over cap area and moment distribution functions, but here we consider qualitatively the spectrum expected from a multitude of very small caps, fewer larger caps, and no caps larger than half the planetary area. Because extremely magnetic materials (*e.g.*, lodestone) tend to be highly localized, we shall not assume total moment is proportional to cap area alone.

At a finite degree n_0, this total spectrum will consist of three attenuated contributions distinguished by cap areas relative to $A_0 = 8\pi r_x^2/[n_0(n_0 + 1)]$. The first is from many relatively small caps ($A_i << A_0$), which are not well resolved by degrees through n_0, and is still increasing in proportion to n^3 near n_0. The second is from fewer large caps ($A_i >> A_0$), which are fairly well resolved, and is a superposition of spectra oscillating with different frequencies and phases near n_0 due to differing half angles θ_i (see (12b)). This contribution amounts to a roughly level value equal to about half the sum of individual envelopes (13). The third contribution is from caps of intermediate area ($A_i \approx A_0$), for which $n_o \approx n^*$, and neither increases as fast as n^3 nor has leveled off.

Similar remarks hold at a higher degree, say $10n_0$ with corresponding area of about $10^{-2}A_0$; however, some caps small compared with A_0 will be of intermediate area compared with $10^{-2}A_0$

and some caps intermediate compared with A_0 will be large compared with $10^{-2}A_0$. The number of caps contributing to an n^3 increase of the total spectrum therefore decreases with n itself, so the net effect of these laterally correlated sources is to soften or redden the spectrum below that expected from fully decorrelated point dipoles. Still, this total spectrum is only expected to approximate an unmodulated exponential near and above degrees so high as to correspond to the smallest caps.

It is possible, and arguably likely, that the magnetic spectrum from a multitude of thin, irregularly shaped, magnetized crustal geologic structures resembles that from our ensemble of independent magnetized spherical caps of various sizes and total moments. If so, at low degrees it would resemble the attenuated cubic (5), while at high degrees, near and above the degree n_{max} corresponding to the smallest crustal magnetic structure (say $A_{min} = 8\pi r_x^2/[n_{max}(n_{max} + 1)]$), the cubic modulation gives way to a roughly constant modulation and the spectrum would resemble a plain exponential.

Clearly n_{max} may be much greater than the highest degree N of coefficients that can be reliably estimated from a set of measured data. If so, the fit of a plain exponential to a reliable observational spectrum will tend to underestimate the depth of the magnetic structures due to both compact, intensely magnetized structures and imperfect correlation of elementary sources within each structure. Moreover, the fit of attenuated cubic (5) to the same observational spectrum will tend to overestimate the depth to the magnetized structures due to lateral correlation of elementary sources within each such structure. Source depth may thus be bounded from both above and below in this case.

In retrospect, geometric attenuation of a crustal-source field with radius implies an exponential decay of multipole powers R_n with harmonic degree n. This decay is modulated by a more slowly varying factor $p(n)$ that depends upon the thickness and roughly ellipsoidal shape of the crust and upon the correlation of magnetic sources within the crust. Theoretical magnetic spectra for laterally uncorrelated dipolar sources can be derived analytically, specify $p(n)$, and may approximate the portion of the satellite-altitude spectrum originating in well separated, local geologic structures. Such spectra yield $p(n)$ which, at asymptotically high degrees, are approximately proportional to: n^3 for a shell of either randomly oriented or random polarity crustal-sources; n^2 for a layer or a ball of such sources; and n^1 for a layer of vertically correlated, but laterally decorrelated, sources. Relative to such spectral forms, the lateral correlation of sources within extended structures is thought to shift multipole power from higher to lower degrees. Such correlation can make $p(n)$ roughly constant near and above the very high degrees corresponding to the smallest significant magnetized crustal structure, if not the rock magnetic domains themselves. Yet at low degrees, and for nearly spherical planets with thin crusts, all these modulation factors increase as n^3. A fit of theoretical spectra like (5) to observational spectra should thus indicate the spectral range of a crustal-source field, although it may tend to overestimate source depth due to extended magnetic structures.

4. TERRESTRIAL TESTS

Observational magnetic spectra R_n for Earth, computed via (2) from the coefficients of truncated spherical harmonic models fitted to measured geomagnetic data, were used to test many theoretical crustal spectra $\{R_n\}$ described above. These tests involved fitting theoretical to observational spectra, so coefficients constrained by assumptions about core or crustal-source fields were not used. Initial trials used R_n from the degree 60 model M102189 and the degree 49

model M102389 fitted to Magsat data by *Cain et al.* [1990]. The logarithms of multipole powers were fitted, $\ln(R_n)$, rather than the R_n themselves; moreover, only degrees 16 and above were fitted with elementary spectra (see 4.3).

Square misfit to a log-observational spectrum is reckoned by the sum of squared residuals per degree of freedom, which, when log-multipole powers of degrees n_{min} through N are fitted with P parameters is

$$s^2 = (N - n_{min} + 1 - P)^{-1} \sum_{n=n_{min}}^{N} [\ln(R_n) - \ln\{R_n\}]^2 . \quad (14a)$$

The statistical significance of the residuals can be estimated using the inverse covariance of $\ln(R_n)$ to weight the residuals and is considered enormous due to the high precision of R_n determined by Magsat data analyses. In contrast, deviations from theoretical $\{R_n\}$ of a factor of $e^{\pm 1}$ were anticipated, so our *a priori* covariance of $\ln\{R_n\}$ was the identity matrix. This is thought to dominate the *a priori* residual covariance $\{\ln[R_n/\{R_n\}]\ \ln[R_{n'}/\{R_{n'}\}]\}$ and was used to weight least squares estimation of the parameters describing $\{R_n\}$. This estimation requires computation of the expected parameter covariance, with diagonal elements indicating expected squared parameter uncertainties. Multiplication of such expectation values by s yields *scaled* parameter uncertainty estimates.

Residuals are also summarized by scatter factor F, the exponential of the rms residual

$$F = \exp([s^2(N - n_{min} + 1 - P)/(N - n_{min} + 1)]^{1/2}) . \quad (14b)$$

This gives a typical factor (or fraction) by which theoretical values overestimate (or underestimate) observational multipole powers. Scatter factor F would be 1.00 if all R_n were

fitted perfectly; it would be 2.00 if each R_n was either twice or half the value of $\{R_n\}$ (so $R_n = 2^{\pm 1}\{R_n\}$); *etc.*. Curiously, we found $F < e$ and $s < 1$ in practice.

4.1 Initial Trials

Following *Langel & Estes* [1982], an unmodulated exponential may fit R_n closely for $n \geq 16$. Linear regression to $\ln[R_n(a)]$ for all $n \geq 16$ from models M102189 and M102389 indeed gave small scatter factors of 1.251 and 1.245, albeit leveling *altitudes* of 208 km and 216 km, respectively. Following *Cain et al.* [1989b], one may suggest that multipole powers above some degree represent noise, assume a degree independent noise spectrum at some altitude, estimate the noise amplitude, and subtract it prior to the regression.

Instead we fitted $\ln[R_n(a_E)]$ with the spectrum expected from a shell of randomly oriented dipoles (5). This is equivalent to fitting a line through the log-demodulated spectrum $\ln[R_n(a_E)[n(n + \frac{1}{2})(n + 1)]^{-1}]$. The least squares fit to degrees 16-60 of $\ln[R_n(a_E)]$ from model M102189 gave a shell depth of 63.5 km and a scaled uncertainty of $\pm$12.0 km ($\pm$36.2 km unscaled). For the thin shell of random polarity dipoles, the fit gave a shell depth of 64.1 km. Similar fits to degrees 16-49 of model M102389 gave shell depths of 94.1 $\pm$ 17.4 km and 95.1 km, respectively.

These source shell depths are thought to overestimate true lithospheric source depths. As a check, each of these four thin-shell crustal-source spectra were extrapolated to high degree and summed to predict a root mean square crustal-source magnetic field on the reference sphere of between 122 and 138 nT. Comparison with magnetic observatory biases, coestimated with models of Magsat data, shows this prediction to be too small by a factor of two to three, apparently due to the excessive shell depths. Although the four fits give scatter factors between 1.359 and 1.382, or about half the anticipated value e, the inconsistent and arguably excessive

shell depths indicate that either (*i*) equation (5) is inadequate, perhaps due to laterally correlated sources, (*ii*) the spectra fitted are not purely crustal, perhaps due to ionospheric fields and noise, or both. The first interpretation is plausible; indeed, the fit of our proxy for lateral source correlation, the spectrum for a ball of random dipoles, to $\ln(R_n)$ of degrees 16-49 from M102389 gives a 6375.4 $\pm$ 15.3 km source radius that differs insignificantly from Earth's equatorial radius. We must, however, consider the second.

4.2 Noise and Model Noise Spectra

For zero mean, uncorrelated noise in the radial magnetic component of mean square amplitude $\{N_r^2\}$ on a shell of radius q, $\{N_r(q)\}$ is zero, as is $\{N_r(q,\theta,\phi)\ N_r(q,\theta',\phi')\}$ unless (θ,ϕ) equals (θ',ϕ'), in which case it is $\{N_r^2\}$. The magnetic spectrum expected when L samples of such noise are (mis-)represented as a single internal potential field,

$$\{R_n(r)\}^{\text{NOISE}} = (L\{N_r^2\}/4\pi)\frac{(2n+1)^2}{n+1}(q/r)^{2n+4}, \qquad (15a)$$

is not independent of degree n at any radius (also see McLeod [1996] and note (15a) with $q = a$ is akin to (9b) with $r_x+d = a$ and $r_x-d = 0$). If the noise is redistributed throughout a thick spherical layer, however, integration of (15a) shows that, for degrees large compared with the radius-to-thickness ratio of the layer, the noise spectrum approaches a plain exponential which levels off at the top of the layer.

Of course, observational R_n computed from a finite number of Gauss coefficients estimated via a thoroughly over-determined least squares fit to satellite magnetic measurements should suffer much less measurement noise than (15a) might suggest. This is because random measurement errors vary in time, change between adjacent measurements along each ground

track, change between adjacent tracks, and thus tend to produce canceling contributions to the model coefficients. Indeed, by the central limit theorem, expectation coefficients $\{g_n^m\}$ and $\{h_n^m\}$ from such noise alone are zero to within $\pm[\{R_n(a)\}^{NOISE}(2n+1)^{-1}L^{-2}]^{1/2}$. The *model* noise spectrum due to L measurements afflicted by such noise is therefore expected to be down by L^{-2}:

$$\{R_n(r)\}^{MODEL}_{NOISE} = (\{N_r^2\}/4\pi L)\frac{(2n+1)^2}{n+1}(q/r)^{2n+4}. \qquad (15b)$$

Unlike random measurement noise, theoretical spectra (5-9) and their random polarity counterparts are not reduced by L^{-2} because crustal signals measured far above the sources remain correlated (along and across tracks), even if the sources are not.

For noise above the reference sphere ($q > r = a$), reference noise spectra (15) increase monotonically with n. If the noise is uncorrelated with crustal signal, its spectrum can be subtracted from observational $R_n(a)$. This correction removes more power at higher than at lower degrees; therefore, a fit of spectrum (5) to a corrected observational spectrum will yield a smaller source shell radius than obtained without correction. The excessive source shell depths found above are therefore not attributed to random measurement noise. Demodulation for thickness factors from (6) or (9c) also reduces mean source radius, while ellipticity factors differ negligibly from unity at degrees as low as 60.

The 0.091 nT^2 noise level of *Cain et al.* [1989b], obtained from $n > 50$ of a numerical integration model [*Cain et al.*, 1989a], implies a rss contribution to a degree 60 field model of about 2.3 nT at 420 km altitude. This is about the rss error expected from uniformly distributed Magsat attitude errors of at most 20" in the ambient field. Yet (15b) makes it doubtful that such errors afflict a least squares model fitted to over 49,000 select Magsat data, such as M102389.

The noise level might instead be due to binning data from very different altitudes prior to numerical integration; if so, it also ought not afflict M102389. The aliasing of any signal in the degree 50-60 coefficients of M102189, which were omitted from M102389, changes R_n but slightly, as shown by the small scatter factor (1.0248) between the models through degree 49.

The possibility of aliasing ionospheric signal remains. *Cain et al.* [1989a] were careful to apply long wavelength mean ionospheric field corrections to separated dawn and dusk Magsat data, but intermediate and short wavelength mean ionospheric signals remain in the data, as do deviations from the mean. The former arguably arise from mean auroral and equatorial electrojets, near-terminator Sq, and perhaps other currents. If so, they should be correlated in dip latitude and magnetic local time, partially decorrelated in Earth-fixed coordinates, yet, like deviations from the mean, strongly correlated along short arcs of the near polar dawn-dusk orbit. If not explicitly parameterized, such fields might contribute more to R_n than (15b) would suggest, and perhaps in a different way.

4.3 Second Trials and Core-Souce Spectrum

Unintended ionospheric source contributions to R_n should be reduced by a more comprehensive geomagnetic field model such as CMP3 [*Sabaka et al.*, 2000], which uses Magsat, POGO, and observatory data to coestimate parameters describing: the main geomagnetic field through degree and order 65; secular variation; the ionospheric field due to Sq, including the equatorial electrojet, and field aligned currents; and magnetospheric source fields. In particular, the use of quasi-dipole coordinates enables efficient separation of narrow scale mean ionospheric-source fields from similarly narrow scale crustal-source fields. Here we use only the main field coefficients at reference epoch 1980, centered on the high precision Magsat data.

The log-observational multipole powers for degrees 16-65 of model CMP3 were fitted in the second set of trials. For the spectrum expected from a shell of randomly oriented dipoles (5), the least squares fit to $\ln[R_n(a_E)]$ gives: a source shell depth of 5.6 km below the 6371.2 km reference sphere, an anticipated uncertainty of $\pm$31.2 km, and a scaled uncertainty of $\pm$13.2 km. The fit with a thin shell of random polarity dipoles gives a source shell depth of 6.3 km with a scaled uncertainty of $\pm$13.3 km. These source depths are thought to approximate true crustal source depths; however, they can be increased by source-layer thickness corrections and/or noise corrections. The large scatter factor ($F = 1.52$) may in part be due to partially correlated sources distributed in a roughly oblate spheroidal annulus with a bi-modal distribution of layer thickness. Indeed, we find a systematic increase in source shell depth with the choice of maximum $N < 65$ fitted that is consistent with lateral source correlation.

A core-source magnetic spectrum is needed to complete spectral separation of crustal from core-source fields. The theoretical core-source spectrum for Earth's magnetic field used here generalizes relations advanced by Stevenson (1983) and McLeod (1996) and is

$$\{R_n(a)\}_c = K_c \frac{n + \tfrac{1}{2}}{n(n+1)} (c_m/a)^{2n+4} . \qquad (16)$$

Linear regressions to $\ln[n(n+1)R_n(a)/[n+\tfrac{1}{2}])$ for degrees 1 through N of model CMP3 yield magnetic estimates of the core radius c_m. The estimates are listed in Table 1 along with square misfit s^2 for N data fitted with two parameters (14a), scaled uncertainty, and error relative to seismologic core radius of 3480 km. As N increases misfit tends to decrease to the minimum at degree 12 and estimated core radius remains quite stable at 3.5 Mm. As N is increased to 13 and then 14, however, misfit increases and then decreases, while c_m begins a monotonic increase.

Both misfit and c_m climb steadily as N is increased to 15 and above. Evidently, non-core source fields contribute to R_n for $n \geq 13$ and markedly so for $n \geq 15$. Moreover, errors in c_m are statistically significant for $N \geq 13$ in that they exceed scaled uncertainties. From Table (1) we infer that: (i) a core-source field dominates the geomagnetic spectrum at degrees 1 through 12; (ii) non-core-source fields contribute significantly to this spectrum at degrees 13 and above; and (iii) non-core-source fields dominate the spectrum at degree 16 and above.

Curiously, with the exception of a spherical ball of measurement noise, which ought not be represented as a potential field, none of the magnetic spectra derived for measurement noise, a crustal-source field, or a core-source field, give the unmodulated exponential suggested by *Lowes* [1974] and assumed by many workers (see Appendix).

5. APPLICATION TO EARTH AND MARS

Figure 1 shows spatial magnetic power spectra of Earth (solid circles through degree 65) and Mars (crosses through degree 90) near the planetary surfaces. The spectrum for Earth, shown at geocentric radius 6371.2 km and epoch 1980, is computed directly from the coefficients of model CMP3 by *Sabaka et al.* [2000]. The spectrum for Mars, shown at areocentric radius 3393.5 km, is computed from the equivalent source model of binned Mars Global Surveyor data by *Purucker et al.* [2000]; the 1°x1° bins are but 10 km in radial extent. The radial field component from that model, evaluated on a 0.5° regular mesh at satellite altitude 3593.5 km, was used to compute spherical harmonic coefficients through degree and order 90, and then 120, via numerical integration (accurate to sixth order in $\Delta\theta$ and to 10 ppm rms in radial field). These coefficients are used to calculate the R_n at altitude, which are then downwardly continued 200 km and shown

in Figure 1. Due to gaps in the low altitude data coverage, we have some reservations about the observational spectrum above degree 40 or 50.

Visual examination of Fig. 1 suggests Earth's magnetic spectrum is dominated by a core source field for degrees 1-12 and by a crustal source field for degrees 16-65. The spectrum for Mars shows no clear sign of a core source field. Moreover, it is not consistent with a degree-independent spectrum at any radius: a line fitted through the low degrees would predict far more power at high degrees than is observed, while a line fitted through the high degrees would predict far more power at low degrees than is observed. A sum of unmodulated exponential forms for R_n is therefore not consistent with this observational spectrum for Mars. The need to modify plain exponential crustal spectra of *Langel & Estes* [1982] and *Cain et al.* [1989b] along the lines of (5) is clear.

5.1 Mars

The two parameter curve fitted through degrees 1-90 of Mars' magnetic spectrum (crosses) shown in Fig. 1 is that expected from a spherical shell of random dipoles (5a). The estimated shell radius is 3342.8 km; the scatter factor is 1.60. The estimated shell depth is 46.7 $\pm$ 6.8 km below the mean planetary radius (unscaled uncertainty). The spectrum from a shell of random polarity field aligned dipoles gives a scatter factor of 1.63 and a shell depth of 47.7 $\pm$ 6.8 km. The difference in scatter seems unimportant; indeed, the scatter exceeds that obtained fitting the same spectral form to degrees 16-65 of terrestrial spectrum CMP3.

The decorrelated source shell is below the equivalent source shell at 3393.5 km; the latter sources are evidently correlated by the fit to MGS data, so it can be argued that the true sources are at depths less than or equal to 50 km. As anticipated from laterally correlated sources, a somewhat smaller scatter factor of 1.40 is obtained when the observational spectrum for degrees

1-90 is fitted with our proxy quadratic form (appropriate to a ball of random dipoles). The ball radius of 3394.5 $\pm$ 6.9 km is indistinguishable from the 3396.2 km equatorial radius of Mars. Estimated source radii are, however, not very stable to major changes in truncation level. The first and second columns of Table 2 show the systematic increase of shell radius with maximum degree N fitted for randomly oriented and random polarity dipoles, respectively. The third column shows the estimated ball radius as a function of N. The instability is due largely to low degree multipole powers, perhaps because the equivalent source model itself omits design matrix elements corresponding to source-to-measurement separations exceeding 1500 km, hence a 3000 km scale.

Because fields of degree n^* contain considerable structure on scales as small as $[(8\pi a^2/n^*(n^*+1)]^{1/2}$, we expect appreciable errors in coefficients of degrees below 6 and perhaps orders below 8 (using $2\pi a/m$). Moreover, the degree n^* corresponding to twice the typical 111.9 km equivalent source spacing is 76. Truncation of the fit at or near this degree often yields a shallow minimum in square misfit, perhaps because equivalent source fields become laterally correlated on the scale of source-spacing.

The 1500 km cutoff means the potential field at different points is computed from different sources. The spectrum from the equivalent source field computed without the cutoff therefore differs from that obtained with the cutoff, particularly at low degrees. Omission of the cutoff reduces R_1 by a factor of 3.54; the scatter factor between the two spectra for degrees 1-5 is 1.818, but only 1.083 for degrees 6-10. Table 3a shows estimated source-shell radius and misfit s as functions of the range of degrees fitted for the spectrum with the 1500 km cutoff (first two columns) and without the cutoff (second pair of columns). Table 3b shows the corresponding

quantities for the ball of random dipoles - our proxy for laterally correlated sources. The tabulated s are based on two rather than four parameters.

For the arguably safe degrees 6-76 of the spectrum without the 1500 km cutoff, the shell model and unscaled uncertainties give

$$\{R_n(a)\}_{\text{Mars}} = (0.3525 \pm 0.0956)\, n\, (n + \tfrac{1}{2})(n + 1)$$
$$[(3343.6 \pm 9.7)/3393.5]^{2n-2} \quad (\text{nT})^2 \quad , \tag{17a}$$

a scatter factor of 1.33, and a slightly smaller misfit than does the ball model. For degrees 6-76 of the spectrum with the cutoff, the shell model gives

$$\{R_n(a)\}_{\text{Mars}} = (0.3478 \pm 0.0943)\, n\, (n + \tfrac{1}{2})(n + 1)$$
$$[(3344.0 \pm 9.7)/3393.5]^{2n-2} \quad (\text{nT})^2 \tag{17b}$$

and a scatter factor of 1.34.

Undulations in the observational spectrum also cause fluctuations in misfit as a function of harmonic degrees fitted. The undulations in the spectral domain are thought to be a modulation resulting from the famous spatial confinement of Mars' strongest magnetic features to a region of the ancient southern highlands, as discovered by Mars Global Surveyor [*Acuna et al.,* 1999; *Connerney et al.,* 1999]. The strong lateral correlations evident in magnetic maps of Mars confirm that deviations from the decorrelated shell spectrum (17) are of high statistical and planetological significance. Yet our decorrelation shell depth of 46 km provides strong support for the shallower values used by *Connerney et al.* [1999] to model individual anomalies with laterally correlated magnetized slabs.

5.2 Earth

The curve fitted through terrestrial spectrum shown in Figure 1 is the sum of a core-source spectrum (16) and that expected from a spherical shell of random dipoles (5). To obtain this

curve, we rely on the identification of some non-core fields at degrees greater than 12 (see 4.3). The initial fit of core spectrum (16) to degrees 1-12 of the CMP3 spectrum is subtracted from the higher degree multipole powers. Shell spectrum (5b) is then fitted to degrees n_{min} through N. This preliminary crustal spectrum is used to correct the degrees 1-12 for a crustal-source field. The core spectrum is then re-estimated, and the procedure repeated. The best fit to the $\ln(R_n)$ is obtained for $n_{min} = 16$, $N = 65$ and is

$$\{R_n(a)\}_{\text{Earth}} = (4.4904 \pm 0.8718) \times 10^{10} \frac{n + \frac{1}{2}}{n(n+1)} [(3512.5 \pm 63.6)/6371.2]^{2n+4}$$
$$+ (1.1354 \pm 0.2120) \times 10^{-3}\, n\,(n + \tfrac{1}{2})(n + 1)[6366.7 \pm 13.5)/6371.2]^{2n-2}\ (\text{nT})^2 \qquad (18)$$

with scaled uncertainties based on 5 parameters (to include n_{min}). Note that model spectrum (18) omits correlation between core and crustal source fields, as well as laterally correlated crustal source fields. For these reasons, observational multipole powers of intermediate degrees 13, 14 and 15 were not used to estimate amplitudes and source radii in (18); however, the prediction errors of (18) for intermediate degrees are included in the misfit, the determination of $n_{min} = 16$, and the uncertainties. Model spectrum (18) underestimates the observational spectrum in the overlap region. This may in part be due laterally correlated magnetization on the scale of continents and ocean basins augmenting the signal from core and other crustal sources.

6. SUMMARY

The spatial magnetic power spectra of Earth, as obtained from the comprehensive model of *Sabaka at al.* [2000], shows clear signs of two distinct classes of internal sources: a core source field and a crustal source field. Spectral analysis shows harmonic degrees 1-12 to be dominated by sources in a core of estimated radius 3512 $\pm$ 64 km; degrees 16-65 are fitted to within a

typical factor of 1.5 by random sources on a crustal shell of radius 6366.7 $\pm$ 13.5 km. Spatial power at intermediate degrees 13, 14, 15 exceeds that expected from the sum of simple core and crustal spectra, perhaps due to crustal sources correlated over continental scales. The magnetic spectrum of Mars obtained from MGS data via the equivalent source model of *Purucker et al.* [2000] shows no sign of a present day core source field; the entire spectrum at degrees 1-90 and the more reliable degrees 6-76 are fitted (to within scatter factors of 1.6 and 1.3, respectively) by random sources on a shell of radius 3344 $\pm$ 10 km. The same theoretical form for a crustal source spectrum fits the observational spectra of both planets better than anticipated, with Mars having a deeper, and more strongly magnetized crust than Earth. Indeed, from the amplitudes A_x^I and shell depths, the ratio of rss magnetic dipole moment per unit area $(K\{M^2\})^{1/2}(4\pi\mu_0 r_x^2)^{-1}$ for Mars' crust to that for Earth's crust is about 9.6 $\pm$ 3.2. We stress that both planetary spectra show very significant deviations from these theoretical forms. These deviations are attributed to physically significant fluctuations in Earth's core source field and to laterally correlated sources in the magnetic lithospheres of Earth and of Mars.

Acknowledgment: This work supported by the National Aeronautics and Space Administration via RTOP 921-622-70-55.

APPENDIX: Unmodulated Spectra

Following *Lowes* [1974], and for comparison with Table 1, linear regressions to $\ln[R_n(a_E)]$ for degrees 1 through N of model CMP3 yield estimates of spectral "leveling radius" shown in Table A.1, alongside square misfit, scaled uncertainty, and the offset of the leveling radius from the core-mantle boundary. The fit is not as close as shown in Table 1 due to omission of the modulation factor; moreover the leveling radius is unstable, tends to increase with N, and differs significantly from the core radius.

Following *Langel & Estes* [1982], dipole power can be excluded to tighten the fit to the low degree non-dipole spectrum. Table A.2 shows the resulting leveling radii along with square misfit (for N-3 degrees of freedom), scaled uncertainty, and the offset from the CMB. Table A.2 shows less misfit than either Table A.1 or Table 1; yet the leveling radius is much less stable than c_m. Indeed, non-dipole leveling radius decreases from 4.1 Mm to 3.2 Mm as N increases from 4 to 8, remains near 3.3 Mm as N increases from 8 to 12, then increases with N as non-core source contributions are fitted. The error of mistaking leveling radius for core radius is statistically significant for $14 \geq N \geq 8$ in that the offset exceeds scaled uncertainty. The agreement at degrees 15 and 16 appears fortuitous. We infer that an unmodulated exponential fits the low degree non-dipole spectrum quite closely, but is not as reliable an indicator of core radius, hence predominantly core-source field, as is (16). Degrees 13, 14, and 15 still include some core-source contribution. As with the purely exponential spectrum itself, theoretical justification for excluding dipole power remains elusive.

REFERENCES

Acuna, M.A., J.E.P. Connerney, N.F. Ness, R.P. Lin, D. Mitchell, C.W. Carlson, J. McFadden, K.A. Anderson, H. Reme, C. Mazelle, D. Vignes, P. Wasilewski, and P. Cloutier, Global Distribution of Crustal Magnetization Discovered by Mars Global Surveyor MAG/ER Experiment. *Science*, 284, 790-793, 1999.

Connerney, J.E.P., M.H Acuna, P.J. Wasilewski, N.F. Ness, H. Reme, C. Mazelle, D. Vignes, R.P. Lin, D.L. Mitchell, and P.A. Cloutier, Magnetic Lineations in the Ancient Crust of Mars. *Science*, 284, 794-798, 1999.

Cain, J.C., Z. Wang, C. Kluth, and D.R. Schmitz, Derivation of a geomagnetic model to n=63, *Geophys. J.*, 97, 431-441, 1989a.

Cain, J.C., Z. Wang, D.R. Schmitz, and J. Meyers, The geomagnetic spectrum for 1980 and core-crustal separation. *Geophys. J.*, 97, 443-447, 1989b.

Cain, J.C., B. Holter, and D. Sandee, Numerical experiments in geomagnetic modeling. *J. Geomagn. Geoelectr.*, 42, 973-987, 1990.

Jackson, A., Accounting for crustal magnetization in models of the core magnetic field. *Geophys. J. Int.*, 103, 657-673, 1990.

Langel, R.A., The Main Field, in *Geomagnetism*, Vol. 1., J.A. Jacobs, ed., Academic Press, 627pp, 1987.

Langel, R.A., and R.H. Estes, A geomagnetic field spectrum. *Geophys. Res. Lett.*, 9, 250-253, 1982.

Lowes, F.J., Mean square values on the sphere of spherical harmonic vector fields. *J. Geophys. Res.*, 71, 2179, 1966.

Lowes, F.J., Spatial power spectrum of the main geomagnetic field and extrapolation to the core. *Geophys. J. R. astr. Soc.* 36, 717-730, 1974.

McLeod, M.G., Spatial and temporal power spectra of the geomagnetic field. *J. Geophys. Res.*, 101, 2745-2763, 1996.

Nerem, R.S., F.J. Lerch, J.A. Marshall, E.C. Pavlis, B.H. Putney, B.D. Tapley, R.J. Eanes, J.C. Ries, B.E. Schultz, M.M. Watkins, S.M. Klosko, J.C. Chan, S.B. Luthcke, G.B. Patel, N.K. Pavlis, R.G. Williamson, R.H. Rapp, R. Biancale, and F. Nouel, Gravity Model Developments for TOPEX/POSEIDON: Joint Gravity Models 1 and 2. *J. Geophys. Res.* 99, 24,421-24,447, 1994.

Purucker M., D. Ravat, H. Frey, C. Voorhies, T. Sabaka, and M. Acuna, An altitude-normalized magnetic map of Mars, *Geophys. Res. Lett.* 27, 2449-2452, 2000.

Sabaka T.J., N. Olsen, and R.A. Langel, A Comprehensive Model of the Near-Earth Magnetic Field: Phase 3. NASA Technical Memorandum 2000-209894, 75pp, 2000.

Smith, D., M. Zuber, S. Solomon, R. Philips, J. Head, J. Garvin, W. Bannerdt, S. Muhleman, G. Pettengill, G. Neumann, F. Lemoine, J. Abshire, O. Aharonson, C. Broawn, S. Hauck, A. Ivanov, P. McGovern, H. Zwally, and T. Duxbury, The Global Topography of Mars and Implications for Surface Evolution. *Science, 284*, 1495-1503, 1999.

Stevenson D.J., Planetary magnetic fields. *Rep. Prog. Phys., 46*, 555-620, 1983.

Voorhies, C.V., Elementary Theoretical Forms for the Spatial Power Spectrum of Earth's Crustal Magnetic Field, NASA Technical Paper 1998-208608, 38pp, 1998.

TABLES FROM TEXT

Table 1: Core radius estimates from model CMP3 and error relative to seismologic estimate

Degrees Fitted	s^2	Core Radius km	Error km (%)
1-4	0.7207	3467 ± 658	- 13 (0.37)
1-5	0.4815	3498 ± 384	+ 17 (0.50)
1-6	0.3612	3503 ± 252	+ 23 (0.66)
1-7	0.2899	3520 ± 179	+ 40 (1.15)
1-8	0.2786	3431 ± 140	- 49 (1.41)
1-9	0.2821	3512 ± 120	+ 32 (0.91)
1-10	0.2479	3501 ± 96	+ 21 (0.60)
1-11	0.2214	3510 ± 79	+ 30 (0.87)
1-12	0.1994	3513 ± 66	+ 33 (0.96)
1-13	0.2046	3548 ± 59	+ 68 (1.95)
1-14	0.1996	3570 ± 53	+ 90 (2.60)
1-15	0.2537	3619 ± 54	+139 (4.01)
1-16	0.3826	3685 ± 62	+205 (5.90)
1-17	0.6817	3776 ± 77	+296 (8.51)
1-18	0.9669	3862 ± 86	+382 (11.0)

Table 2. Estimated source radius for models of Mars' magnetic spectrum and unscaled uncertainty in km.

Degrees Fitted	Shell of Random Dipoles	Shell of Random Polarity	Ball of Random Dipoles
1- 5	2357 ±373	2311 ±365	2764 ±437
1-10	2980 ±164	2955 ±163	3293 ±181
1-15	3195 ± 95	3180 ± 95	3438 ±103
1-30	3267 ± 34	3261 ± 34	3405 ± 36
1-45	3304 ± 19	3302 ± 19	3402 ± 20
1-60	3326 ± 12	3324 ± 12	3401 ± 13
1-75	3334 ± 9	3332 ± 9	3395 ± 9
1-90	3343 ± 7	3342 ± 7	3394 ± 7

Table 3a. Estimated shell radius for random dipoles model of Mars' magnetic spectrum in km, unscaled uncertainty, and misfit

Degrees Fitted	With Cutoff r_x	With Cutoff s	Without Cutoff r_x	Without Cutoff s
1-90	3343 ± 7	0.4759	3344 ± 7	0.3806
1-76	3334 ± 9	0.4841	3336 ± 8	0.3765
6-90	3350 ± 7	0.2984	3350 ± 7	0.2942
6-76	3344 ±10	0.2987	3344 ±10	0.2921

Table 3b. Estimated ball radius for random dipoles model of Mars' magnetic spectrum in km, unscaled uncertainty, and misfit.

Degrees Fitted	With Cutoff r_x	With Cutoff s	Without Cutoff r_x	Without Cutoff s
1-90	3395 ± 7	0.3420	3396 ± 7	0.3054
1-76	3395 ± 9	0.3685	3397 ± 9	0.3269
6-90	3394 ± 8	0.3047	3394 ± 8	0.2944
6-76	3394 ±10	0.3309	3393 ±10	0.3167

FIGURE CAPTION

Figure 1: Mean square magnetic induction on sphere of radius a, $R_n(a)$ in nT^2, from harmonics of degree n for Earth (solid circles, a_E = 6371.2 km [*Sabaka et al.*, 2000]) and Mars (crosses, a_M = 3393.5 km [*Purucker et al.*, 2000]). For Earth, curve shows sum of spectra from core sources (3512.5 ± 63.5 km radius) and crustal source shell of random dipoles (4.5 ± 13.5 km below a_E). For Mars, curve shows spectrum from crustal source shell of random dipoles (50.7 ± 6.8 km below a_M). Evidently, Mars' core field has decayed away, yet its magnetic crust is deeper and far stronger than Earth's.

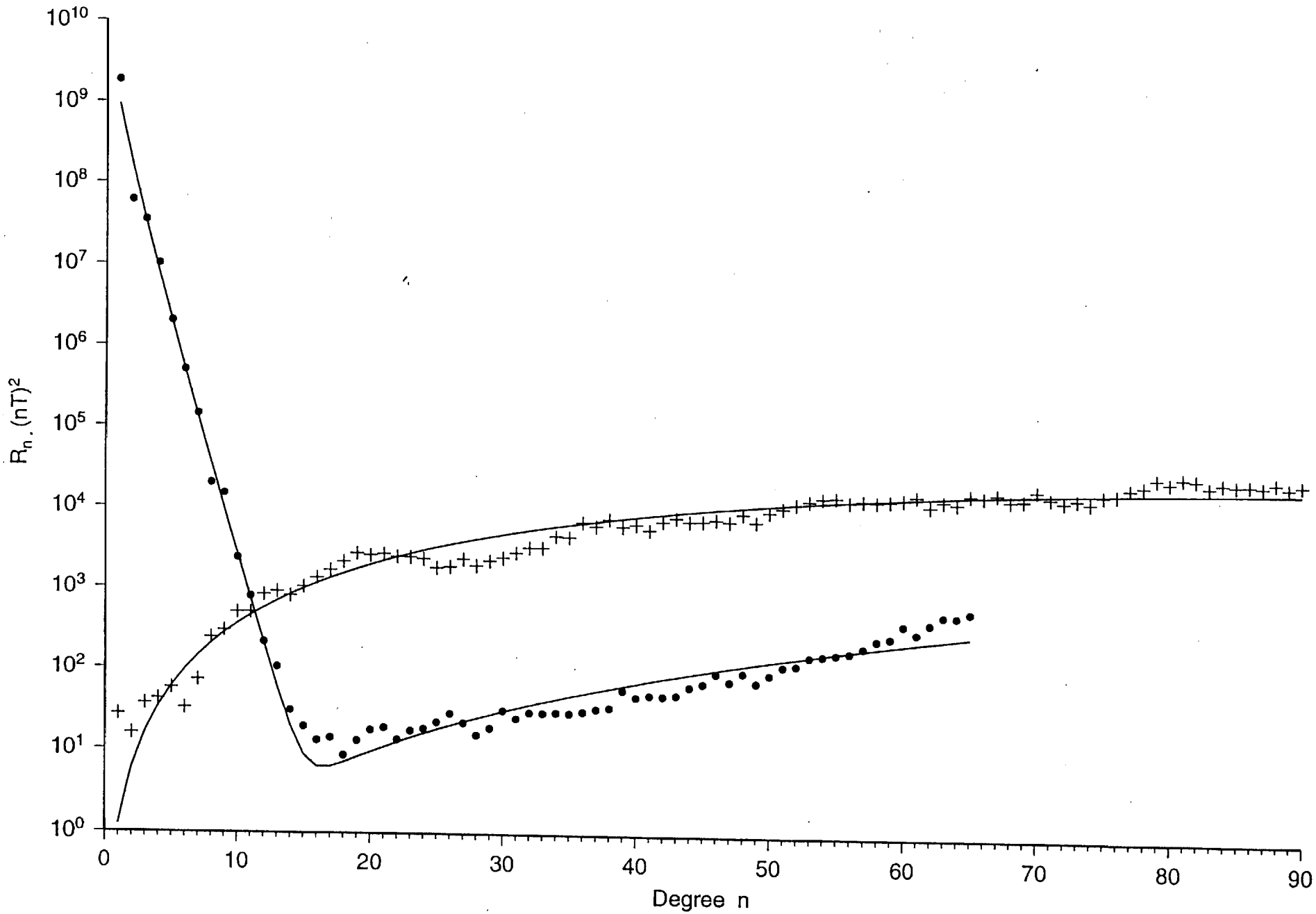
10^{10}
10^{9}
10^{8}
10^{7}
10^{6}
10^{5}
10^{4}
10^{3}
10^{2}
10^{1}
10^{0}
R_n, $(nT)^2$
0
10
20
30
40
50
60
70
80
90
Degree n

TABLES FROM APPENDIX

Table A.1: Leveling radius from model CMP3

Degrees Fitted	s^2	Level Radius km	Offset km (%)
1-4	0.9093	2843 ± 606	- 637 (18.3)
1-5	0.6230	2946 ± 368	- 534 (15.4)
1-6	0.4781	3010 ± 249	- 470 (13.3)
1-7	0.3984	3073 ± 129	- 407 (11.7)
1-8	0.3416	3033 ± 137	- 447 (12.9)
1-9	0.3834	3137 ± 125	- 344 (9.87)
1-10	0.3389	3154 ± 101	- 326 (9.36)
1-11	0.3163	3186 ± 85	- 294 (8.44)
1-12	0.2947	3209 ± 73	- 271 (7.78)
1-13	0.3252	3259 ± 69	- 221 (6.35)
1-14	0.3363	3296 ± 63	- 184 (5.29)
1-15	0.4312	3356 ± 66	- 124 (3.57)
1-16	0.6178	3430 ± 73	- 50 (1.44)
1-17	1.0009	3527 ± 87	+ 47 (1.35)
1-18	1.3637	3619 ± 96	+139 (3.99)

Table A.2: Leveling radius from model CMP3

Degrees Fitted	s^2	Level Radius km	Offset km (%)
2-4	0.0797	4080 ± 407	+600 (17.2)
2-5	0.1480	3592 ± 309	+112 (3.21)
2-6	0.1309	3420 ± 196	- 60 (1.72)
2-7	0.1034	3369 ± 129	- 111 (3.20)
2-8	0.1522	3226 ± 119	- 254 (7.28)
2-9	0.1663	3313 ± 104	- 167 (4.79)
2-10	0.1449	3296 ± 81	- 184 (5.30)
2-11	0.1280	3307 ± 65	- 173 (4.97)
2-12	0.1143	3313 ± 54	- 167 (4.80)
2-13	0.1334	3355 ± 51	- 125 (3.59)
2-14	0.1387	3384 ± 47	- 96 (2.77)
2-15	0.2128	3441 ± 53	- 39 (1.12)
2-16	0.3686	3516 ± 64	+ 36 (1.02)
2-17	0.7063	3617 ± 82	+137 (3.93)
2-18	1.0193	3711 ± 93	+231 (6.64)